Studies on the nucleation of MBE grown III-nitride nanowires on Si*

Yanxiong E(鄂炎雄), Zhibiao Hao(郝智彪)†, Jiadong Yu(余佳东), Chao Wu(吴超), Lai Wang(汪莱), Bing Xiong(熊兵), Jian Wang(王健), Yanjun Han(韩彦军), Changzheng Sun(孙长征), and Yi Luo(罗毅)

Tsinghua National Laboratory for Information Science and Technology, Department of Electronic Engineering, Tsinghua University, Beijing 100084, *China*

(Received 3 February 2016; revised manuscript received 10 September 2016; published online 30 November 2016)

GaN and AlN nanowires (NWs) have attracted great interests for the fabrication of novel nano-sized devices. In this paper, the nucleation processes of GaN and AlN NWs grown on Si substrates by molecular beam epitaxy (MBE) are investigated. It is found that GaN NWs nucleated on *in-situ* formed Si_3N_4 fully release the stress upon the interface between GaN NW and amorphous Si_3N_4 layer, while AlN NWs nucleated by aluminization process gradually release the stress during growth. Depending on the strain status as well as the migration ability of III group adatoms, the different growth kinetics of GaN and AlN NWs result in different NW morphologies, i.e., GaN NWs with uniform radii and AlN NWs with tapered bases.

Keywords: GaN nanowires, AlN nanowires, strain, nucleation

PACS: 61.46.Km, 61.72.Hh, 64.60.Q– **DOI:** 10.1088/1674-1056/26/1/016103

1. Introduction

III-nitride nanowires (NWs) are considered as promising semiconductor materials for the fabrication of nano-lasers,[1] photocatalysis devices,[2] optical sensors,[3] and single photon emitters[4] due to their perfect crystalline quality, low-dimensional characteristics, and compatibility with many kinds of substrates. Therefore, GaN NWs, AlN NWs, and their alloys have attracted intense research interests. The spontaneous growth of III-nitride NWs by molecular beam epitaxy (MBE) exhibits great advantages for the fabrication of those devices, since it does not require the use of any catalysts, substrate pre-patterning, or masks which inevitably introduce impurities and more complexity of the process.

Generally, the spontaneous growth of III-nitride NWs includes two phases: the nucleation phase and the growth phase. The nucleation phase plays an important role in the self-induced three-dimensional formation of NWs. A few experimental and theoretical works[5–7] about the GaN NW nucleation mechanisms have been reported. It is believed that the nucleation begins with an incubation period, during which the Ga and N sources react to form initial crystal islands until their sizes reach a critical value; after that the transformation from nuclei to NWs occurs driven by the anisotropy of the surface energy. However, the nucleation process is still not fully understood so far, especially the strain status of the NW nuclei formed under different nucleation conditions as well as its influence on the NW growth.

In this work, GaN and AlN NWs are spontaneously grown on Si_3N_4-buffered Si (111). GaN NWs nucleate directly on *in-situ* formed Si_3N_4, while AlN NWs nucleate from the AlN islands formed by an aluminization process.[8] Investigation on the strain status of GaN and AlN NWs reveals strain-free GaN NW nuclei and strained AlN NW nuclei. Finally, the difference between the growth kinetics of GaN and AlN NWs are discussed.

2. Experiments

All NW samples were grown on Si (111) substrates in a plasma-assisted MBE (PAMBE) system (SVTA 35N). Before being put into the MBE chamber, the Si substrates were treated by a standard RCA cleaning process. Then the substrates were outgassed at 940 °C for 15 min in the growth chamber. Before the growth, the substrates were nitridated at 900 °C to form Si_3N_4 on the surface. In the case of GaN NWs, the substrate temperature was reduced to 750 °C after nitridation, then the NWs were grown with the Ga flux fixed at 6.4×10^{-8} Torr and the N_2 flow rate fixed at 1.7 sccm under 375 W RF power. In the case of AlN NWs, the aluminization process was performed at 900 °C after nitridation. Then the AlN NWs were grown at 960 °C, with the Al flux fixed at 8.1×10^{-8} Torr and the N_2 flow rate fixed at 2.5 sccm under 375 W RF power. The growth procedure was monitored *in-situ* by a reflection high-energy electron diffraction (RHEED) system.

3. Results and discussion

Hestroffer *et al.*[9] have reported that an amorphous Si_3N_4 layer can improve the GaN NW nucleation. In our exper-

*Project supported by the National Basic Research Program of China (Grant No. 2013CB632804), the National Natural Science Foundation of China (Grant Nos. 61176015, 61176059, 61210014, 61321004, and 61307024), and the High Technology Research and Development Program of China (Grant No. 2012AA050601).

†Corresponding author. E-mail: zbhao@tsinghua.edu.cn

© 2017 Chinese Physical Society and IOP Publishing Ltd

iments, the Si(111) surface was nitridated for 120 s until the "8×8" RHEED pattern disappeared, and the Si_3N_4 layer obtained on the Si surface became amorphous.[10] By this method, a very smooth Si_3N_4 surface favoring the migration of Ga adatoms can be obtained. Then GaN NWs were directly grown under N-rich condition, with the appearance of spotty RHEED patterns which indicates the three-dimensional growth of GaN NWs.

Figure 1(a) shows a bird's-eye-view SEM image of the GaN NWs growing vertically on the substrate, and the hexagonal shape of the NWs indicates the wurtzite nature of GaN. The cross-section high resolution transmission electron microscopy (HRTEM) image shown in Fig. 1(b) illustrates that between GaN and Si there is an amorphous Si_3N_4 layer with bright contrast. It is obvious that the GaN NWs nucleate directly on the Si_3N_4 buffer layer, presenting good crystalline quality without any observable defects. Figure 1(c) is a Fourier filtered[11] TEM image of the GaN NW in the area right above the Si_3N_4 surface marked by the red square in Fig. 1(b). The image is quite clear and the distance between c (002) planes is calibrated to be 5.19 Å by averaging the distances at different positions between the marked two planes. The distance is exactly consistent with that of bulk GaN, demonstrating that the GaN crystal on the interface has completely relaxed owing to the poor bonding provided by the amorphous Si_3N_4. Due to the same reason, the NWs are very easy to be moved off the substrate, as the image shows in Fig. 1(a) which is caused by an unintentional scratch during the SEM sample preparation. The high crystalline quality of the GaN NWs is also evidenced by the sharpness of the E_{2h} peak of the Raman spectrum in Fig. 2. The central frequency shift of the E_{2h} peak is 567 cm^{-1}, coinciding with the value reported for bulk GaN.[12] This measurement result further proves that the GaN NWs are free of stress.

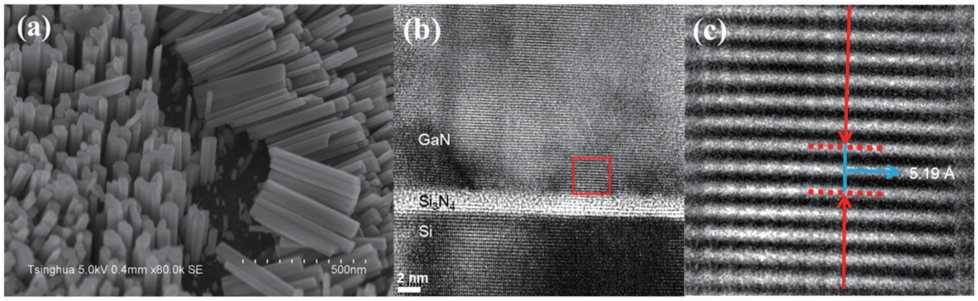


Fig. 1. (color online) (a) A bird's-eye-view SEM image of GaN NWs taken with a 30° angle. (b) A cross-section HRTEM image of a single GaN NW. (c) A Fourier filtered TEM image of the GaN NW in the area marked by the red square in panel (b), the average c (002) plane distance is measured to be 5.19 Å.

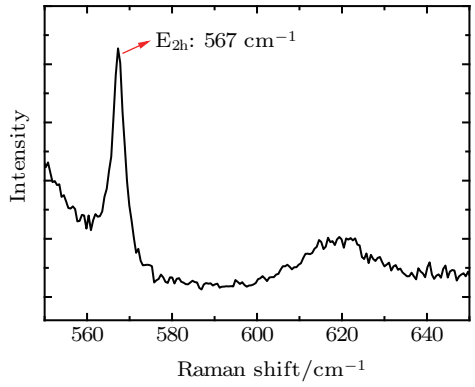


Fig. 2. (color online) Raman spectrum of GaN NWs.

Different from GaN NWs, AlN NWs cannot nucleate directly on Si_3N_4. In order to promote the nucleation of AlN NWs, an aluminization process was introduced. First, a few monolayers of β-Si_3N_4 with "8×8" RHEED patterns were formed after nitridation for 60 s. Then the N plasma source was turned off, and an Al flux was irradiated for long enough time during which excessive Al adatoms reacted with the β-Si_3N_4 to form AlN islands acting as nuclei of AlN NWs. SEM images of the samples grown with and without aluminization process are shown in Figs. 3(a) and 3(b), respectively, the inset of Fig. 3(a) is an SEM image of the AlN NWs grown after nucleation phase. As revealed by the images, the density of the AlN NWs is lower than that of the GaN NWs while the diameter of the AlN NWs is larger, because of different migration abilities of Al adatoms and Ga adatoms. It is noted that the AlN NWs cannot nucleate without aluminization process, and AlN films with pyramid-like morphology are formed instead, which is similar to the films growing between the NWs in Fig. 3(a). The tapered shape at the base of AlN is seen in Fig. 3(a), which is more clearly shown in the inset, while the GaN NWs show uniform shape along the c-axis, demonstrating different growth mechanisms, which will be discussed later below.

Figure 4(a) shows the cross-section HRTEM image of the base area of a single AlN NW. The AlN NW directly grows on Si (111) with no Si_3N_4 between them, which is clear evidence that Al adatoms react with Si_3N_4 during the aluminization process. The upper part of the AlN NW exhibits very good crystalline quality without visible defects, while the lower part

near the AlN–Si interface contains some defects which accommodate the lattice mismatch. Figure 4(b) is a Fourier filtered TEM image of the AlN crystal right above the AlN–Si interface. The distances between *c* (002) planes of the AlN crystal in the lower part and the upper part are calibrated to be 4.66 Å and 4.94 Å, respectively, with lattice deformation of 6.4% and 0.8% along *c*-axis compared to 4.98 Å of bulk AlN. Therefore the AlN crystal in the lower part undergoes moderate tensile stress, while the AlN crystal in the upper area has released most of the stress. The AlN nuclei cannot fully release the stress during the aluminization process due to strong bonding between Si and AlN. As the AlN NWs grow larger, the free surfaces of the NWs assist the release of the strain.

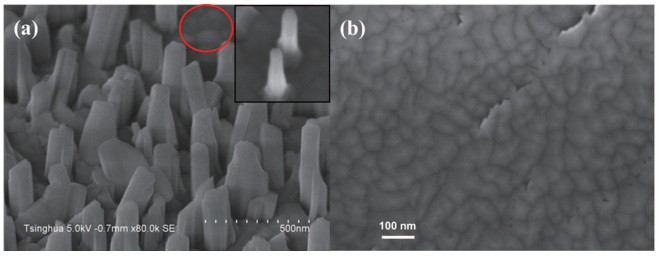


Fig. 3. (color online) (a) A bird's-eye-view SEM image taken with a 30° angle, the red circle highlights the AlN film growing between NWs. The inset is the AlN NWs grown after nucleation, the tapered shape at the base is clearly seen. (b) A plane view SEM image of the sample without aluminization process.

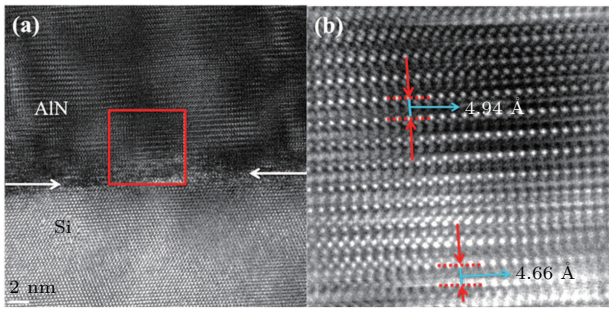


Fig. 4. (color online) (a) A cross-section HRTEM image of the base area of a single AlN NW. (b) A Fourier filtered image of the AlN NW in the area marked by the red square in panel (a), the *c* (002) plane distances in the lower part and the upper part are measured to be 4.66 Å and 4.94 Å, respectively.

The Raman spectrum of the AlN NWs is shown in Fig. 5. Obviously, two sharp E_{2h} peaks at 656 cm^{-1} and 653 cm^{-1}, respectively, are observed. The resolution of the Raman spectrometer is 0.5 cm^{-1}, which is much smaller than the distance between these two peaks. These two peaks always appear in several Raman spectra measured at different positions of the sample, demonstrating that they are not caused by noise. A decrease in the E_{2h} phonon frequency with respect to strain-free AlN indicates tensile strain, and the absolute value of the frequency shift varies linearly with the stress. The amount of stress can be evaluated using the proportionality factor of 4.04±0.3 $cm^{-1}\cdot GPa^{-1}$ for hexagonal AlN, while the peak position for bulk AlN should be at 657 cm^{-1}.[12] Therefore, the two peaks correspond to tensile stresses of 0.25 GPa and 0.99 GPa, respectively (the area we measured is about 5 μm^2, it contains both AlN NWs and AlN films). The Raman spectrum that presents two peaks is also evidence of the AlN films growing between NWs. The free surfaces of the AlN NWs release most of the stress with little residual stress, while the AlN films between the NWs cannot effectively release the tensile stress. Although the NWs and the films are with different polarities according to our previous report,[13] the E_{2h} peak does not change along with polarity.[14] Therefore, the peak at 656 cm^{-1} representing small tensile stress corresponds to the NWs, whereas the peak at 653 cm^{-1} corresponds to the films.

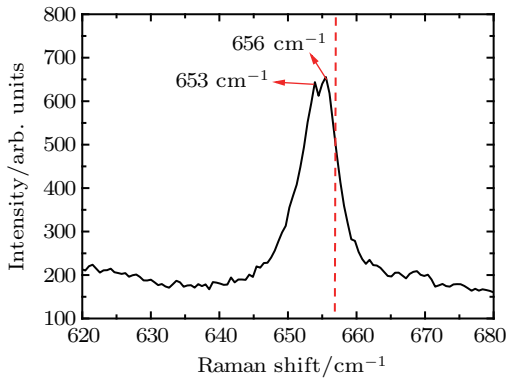


Fig. 5. (color online) Raman spectrum of AlN NWs, the peaks at 656 cm^{-1} and 653 cm^{-1} correspond to the NWs and the films between NWs, respectively. The red dashed line indicates the position of bulk AlN.

The results presented above clearly reveal the difference between the nucleation kinetics of GaN NWs and AlN NWs. The first point to be discussed is related to the migration abilities of Ga and Al adatoms. The potential energy barrier for the migration of Ga atoms on Si_3N_4 is relatively low due to the small Ga–N bond energy. Therefore, the average diffusion length of Ga adatoms is relatively large,[15] which favors the three-dimensional nucleation of NWs. As observed by SEM, the average distance between the GaN NWs is 50–100 nm, which is less than the Ga diffusion length. Therefore, after nucleation, most of the following Ga atoms falling between NWs will be absorbed into the initially nucleated GaN NWs through surface diffusion. The adatoms that do not diffuse to the GaN NWs will nucleate to form new NWs between the initial ones. On the other hand, the average diffusion length of Al adatoms on Si_3N_4 is relatively short because of the large Al–N bond energy which introduces a high potential energy barrier for the Al migration. The average distance between the nuclei formed by aluminization is about 300–500 nm, which is much larger than the diffusion length of Al adatoms.[16] After aluminization nucleation, the AlN islands are surrounded by bare Si, then at the beginning of AlN NW growth, Al and N fluxes are simultaneously irradiated to the substrate, and the bared Si

(111) surface between AlN nuclei is unintentionally nitridated to form Si_3N_4. Thus although part of the Al adatoms migrate to the AlN NW nuclei, AlN films are also formed between NWs on Si_3N_4, as shown in Fig. 4(a). The reason for the formation of films instead of NWs is the crystal polarity. In our previous report,[13] the AlN islands forming after aluminization are N-polar while the AlN films directly grown on Si_3N_4 are Al-polar. It has been reported[17] that under N-rich growth conditions, the $(11\bar{2}n)$ facets are more stable than the (0001) one, whereas the $(112n)$ facets are less stable than the $(000\bar{1})$ one. Thus the N-polar AlN islands prefer to transform to NWs terminated by $(000\bar{1})$ plane. However the Al-polar AlN nuclei tend to form pyramid-like AlN islands terminated by $(11\bar{2}n)$ planes, then the Al-polar AlN pyramids keep growing until coalescence, evidenced by the AlN films on the un-aluminized sample shown in Fig. 3(b) as well as the ones between the AlN NWs shown in Fig. 3(a).

The second point to be discussed is related to the strain status in NWs. It can be observed that each GaN NW has a uniform radius, whereas the AlN NWs frequently show a tapered shape at the base. For the GaN NWs, the stress is fully released upon the interface between GaN NW and amorphous Si_3N_4 layer, thus the NWs exhibit uniform radii along the *c*-axis owing to the uniform radial growth rate. However, the stress in the AlN NW base is not efficiently released, therefore most of the AlN islands suffer from tensile stress at the beginning of growth. The stress hinders the free shape transformation from island to NW, because the stress has to be released during island enlarging with minimized total free energy per unit volume, only after which the shape transformation, mainly driven by the anisotropy of the surface energy, can take place.[5] Moreover the lattice constant in the top of the island is closer to that of bulk AlN, nucleation on the top is preferable due to the relatively low chemical potential,[18] thus the axial growth on the top is faster. The factors discussed above finally result in the tapered shape at the AlN NW base. After the formation of NW, the radius in the upper part becomes uniform along the *c*-axis, just like GaN NWs.

4. Conclusion

The nucleation processes of GaN and AlN NWs grown by MBE have been investigated. The AlN NWs nucleated by aluminization process present strong bonding to the substrate in contrast to the GaN NWs nucleated on Si_3N_4, therefore the AlN NWs cannot fully release the stress as the GaN NWs do. During the enlarging of AlN nuclei, the top parts release tensile stress more efficiently and the axial growth on the top is faster, which results in the tapered shape at the NW base. On the contrary, the fully strain-free GaN NWs show uniform radii.

References

[1] Lu Y J, Kim J, Chen H Y, Wu C, Dabidian N, Sanders C E, Wang C Y, Lu M Y, Li B H, Qiu X, Chang W H, Chen L J, Shvets G, Shih C K and Gwo S 2012 *Science* **337** 450

[2] Wang D, Pierre A, Kibria M G, Cui K, Han X, Bevan K H, Guo H, Paradis S, Hakima A R and Mi Z 2011 *Nano Lett.* **11** 2353

[3] Maier K, Heiwig A, Müller G, Becker P, Hille P, Schörmann J, Teubert J and Eickoff M 2014 *Sensors and Actuators B* **197** 87

[4] Holmes H J, Choi K, Kako S, Arita M and Arakawa Y 2014 *Nano Lett.* **14** 982

[5] Consonni V, Hanke M, Knelangen M, Geelhaar L, Trampert A and Riechert H 2011 *Phys. Rev. B* **83**

[6] Consonni V, Knelangen M, Geelhaar L, Trampert A and Riechert H 2010 *Phys. Rev. B* **81**

[7] Landre O, Bougerol C, Renevier H and Daudin B 2009 *Nanotechnology* **20** 415602

[8] Hu J N, Hao Z B, Niu L, E Y X, Wang L and Luo Y 2013 *Appl. Phys. Lett.* **102** 141913

[9] Hestroffer K, Leclere C, Cantelli V, Bougerol C, Renevier H and Daudin B 2012 *Appl. Phys. Lett.* **100** 212107

[10] Ahn H, Wu C L, Gwo S, Wei C M and Chou Y C 2001 *Phys. Rev. Lett.* **86** 2818

[11] Carlton C E and Ferreira P J 2009 *Microsc Microanal* **15** 736

[12] Kuball M 2001 *Surface and Interface Analysis* **31** 987

[13] E Y, Hao Z, Yu J, Wu C, Liu R, Wang L, Xiong B, Wang J, Han Y, Sun C and Luo Y 2015 *Nanoscale Res. Lett.* **10** 383

[14] Zhong F, Li X H, Qiu K, Yin Z J, Ji C J, Cao X C, Han Q F, Chen J R and Wang Y Q 2007 *Chin. Phys.* **16** 2786

[15] Gotschke T, Schumann T, Limbach F, Stoica T and Calarco R 2011 *Appl. Phys. Lett.* **98** 103102

[16] Banal R G, Funato M and Kawakami Y 2009 *Phys. Status Solidi (c)* **6** 599

[17] Auzelle T, Haas B, Minj A, Bougerol C, Rouvière J L, Cros A, Colchero J and Daudin B 2015 *J. Appl. Phys.* **117** 245303

[18] Schulli T U, Vastola G, Richard M I, Malachias A, Renand G, Uhlik F, Montalenti F, Chen G, Miglio L, Schaffler F and Bauer G 2009 *Phys. Rev. Lett.* **102** 025502